Available online at www.sciencedirect.com

ScienceDirect

Procedia CIRP 136 (2025) 348–353

www.elsevier.com/locate/procedia

35th CIRP Design 2025

Design of a Tendon Driven Virtual Rolling Contact Joint for Deep-Sea Application

Cora Maria Sourkounis[a]*, Henning Wienöbst[a], Jan Peters[a], Tom Kwasnitschka[b], Annika Raatz[a]

[a]*Institute of Assembly Technology and Robotics, Leibniz University Hannover, An der Universität 2, 30823 Garbsen, Germany.*
[b]*GEOMAR Helmholtz Centre for Ocean Research, Wischhofstr. 1-3, 24148 Kiel, Germany.*

* Corresponding author. Tel.: +49 511 762 18206; *E-mail address:* sourkounis@match.uni-hannover.de

Abstract

The "Active Suction Device for Deep Sea Applications" (ASDDSA) project aims to develop a pressure-neutral actuation system for a suction sampler attached to work class or inspection class tethered diving robots to collect sediment samples at depths up to 6000m. The aim of the project includes improving operability, reduce cost and maintenance effort without negatively affecting the vehicle's buoyancy. The actuation system must be scalable and modular to be compatible with various size of host systems. To meet a variety of environmental and operational deep-sea requirements, a tendon driven Virtual Rolling Contact Joint was designed positioning the suction conduit at the center of the prototype. Initial testing under laboratory conditions has provided preliminary proof of concept.

Keywords: Virtual Rolling Contact Joint; Quaternion Join; Tendon Actutation; Marine Robotics; Sediment Sampling

1. Introduction

Suction sampling is a commonly employed technique for acquiring sediment samples from the deep sea. These samples serve as vital resources for investigating and understanding the unexplored regions of the deep-sea floor [1]. To explain the motivation for the ASDDSA project, it is necessary to first outline the current procedure for retrieving sediment samples from the deep sea using a suction sampling system. Initially, the Remotely Operated Vehicle (ROV) must be transported to the target location by a research vessel. This ROV is rated for operations at depths of up to 6000 m and is accompanied by necessary equipment and a crew to operate it in the target area. Given that the ROV can weigh up to 5000 kg, it necessitates the use of an adequately sized vessel for transportation [2] During the expedition, the ROV is submerged to the ocean floor, where a hydraulic titanium manipulator attached to the ROV directs the suction sampling tube, which then collects the required sediments by creating negative pressure. Once all sampling cartridges are filled, the ROV ascends, and the samples are retrieved from the unit. This whole procedure incurs a cost of approximately 1 € per second while the ROV is deployed.

To reduce the costs associated with sediment sampling and thereby make it more accessible to a broader range of researchers, we aim to develop an innovative actuation system for deep-sea sediment sampling in collaboration with the GEOMAR Helmholtz Centre for Ocean Research. The projects long term goal is to utilize a smaller vessel carrying a more lightweight robot, equipped with a cost-effective, actively controlled suction tube. To achieve this goal, the new version of the suction sampling system will be significantly lighter and more compact than traditional manipulators. To minimize costs, the new system will avoid using titanium for its components. Instead, carbon fiber-reinforced polymers and other non-corrosive, non-metallic materials will be employed

In the initial phase of the project, we will develop an actuation system enclosing the suction sampling tube to be integrated into existing ROV. The subsequent step involves

10.1016/j.procir.2025.08.061

miniaturizing the ROV as well to further reduce the overall system's weight.

Deep-sea equipment must contend with extreme conditions, including high ambient pressure, strong water currents, low temperatures, and corrosive environments. These challenges impose specific design requirements on the system. To operate effectively at depths of up to 6000 m, the system must incorporate a pressure-neutral design. Additionally, its components should be scalable in terms of size, layout, and manufacturing processes, with external parts, such as motors, sourced from scalable product lines to accommodate various host ROV sizes. To ensure near-neutral buoyancy, the design should avoid using metal parts, components should allow for easy replacement and seawater hydraulics should be considered over traditional hydraulics to minimize environmental impact

Previous approaches for developing a suitable design involved exploring soft [3], binary [4] and hyper-redundant robotic structures [5]. These investigations revealed that a simple, tendon-driven structure could also be an effective solution, particularly in scenarios where obstacle avoidance and additional degrees of freedom at the robot's tip are not required. This led to the concept of utilizing a tendon actuation, which allows to encapsulate the motors within the ROV. The joint design is inspired by the Virtual Rolling Contact Joint (VRCJ), also known as the Quaternion Joint, as presented by [6].

This paper's contributions are as follows:

- A novel design concept for a deep-sea suction sampler.
- Design optimization based on mathematic model
- Laboratory testing of the prototype under controlled conditions.

2. Concept

The state-of-the-art suction sampling procedure of directing the nozzle with a traditional manipulator arm results in the formation of a large loop in the suction conduit. Positioning the suction conduit at the robot's center minimizes the risk of entanglement. To ensure an adequate bending radius for the conduit, an appropriate joint is required. Another key criterion in evaluating different concepts was the goal of implementing antagonistic actuation. This is crucial for reducing the number of drives needed and enabling energy-efficient operation of the robotic arm.

Various joint designs were evaluated to meet the application's requirements while maintaining a structure that is as simple as possible. Options considered included the omni-wrist [4], a tendon-driven cardan joint [5] and the virtual contact rolling joint. Finally, the concept of the tendon driven VRCJ was chosen for the further development of the robot. It mimics the motion of two spheres rolling without friction and allows for actuation with to opposing pairs of wires.

Fig. 1 illustrates the concept of the VRCJ, adapted to meet the requirements dictated by the intended deep-sea application. It incorporates the sampling conduit at the center of the structure. The bending radius of the joint has been carefully selected to ensure the tube not being damaged.

Fig.1. Concept of the tendon-driven Virtual Rolling Contact Joint

The next section describes the design optimization necessary for achieving slack-free tendon actuation.

3. Design Optimization based on Mathematical Model

To control the VRCJ, a spherical rolling motion is assumed. However, the actual motion follows an elliptical path, which leads to a varying the cable tension. To minimize slack in the drive cables, the elliptical motion of the joint needs to be approximated by a circular rolling motion. This can be achieved by calculating the joint positions for the intended range of motion and fitting a circular arc with a vertically offset center point, as shown in Fig. 2 [6].

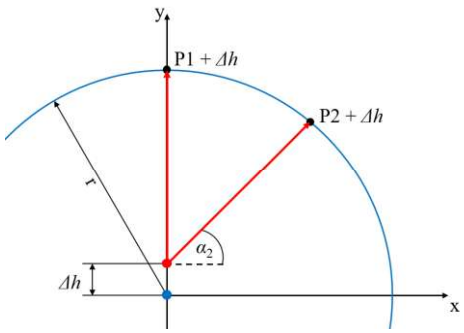

Fig. 2. Fitting of a circular arc through the calculated joint positions.

Since the geometry of the full joint is mathematically over constrained, the motion of a single linkage is described and later combined into the position of the full joint.

To simplify the calculation, a common plane of all segments in a single linkage can be used to create a two-dimensional closing condition. By aligning the unknown distance l_6 along the x axis, the calculation can be further simplified.

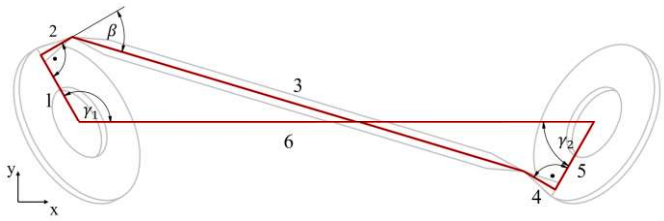

Fig. 3. Simplified representation of the joint reduced to two dimensions

The calculation of the midpoint distance for a single link can be done via a two-dimensional closing condition:

$$\begin{pmatrix} l_6 \\ 0 \end{pmatrix}_6 = \begin{pmatrix} l_1 * \cos\gamma_1 \\ l_1 * \sin\gamma_1 \end{pmatrix}_1 + \begin{pmatrix} l_2 * \sin\gamma_1 \\ -l_2 * \cos\gamma_1 \end{pmatrix}_2 + \begin{pmatrix} l_3 * \cos(\gamma_1 - \beta - 90°) \\ l_3 * \sin(\gamma_1 - \beta - 90°) \end{pmatrix}_3 + \begin{pmatrix} l_4 * \sin\gamma_2 \\ -l_4 * \cos\gamma_2 \end{pmatrix}_4 + \begin{pmatrix} l_5 * \cos\gamma_2 \\ l_5 * \sin\gamma_2 \end{pmatrix}_5 \quad (1)$$

The angles γ_1 and γ_2 can be derived from the bending angle and the rotation relative to the bending plane as shown in Fig. 4.

$$\gamma_1 = \cos^{-1}(-\cos\alpha_1 * \cos\alpha_2) \qquad \gamma_2 = \cos^{-1}(\cos\alpha_1 * \cos\alpha_2) \quad (2)$$

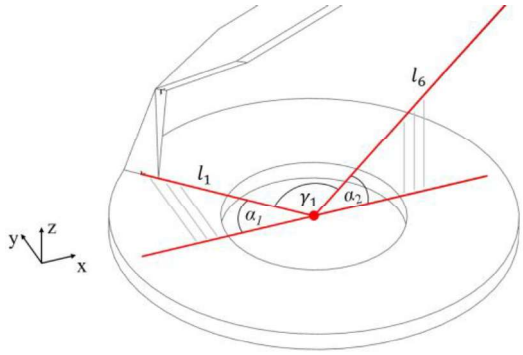

Fig. 4. Angles in the base of the Joint.

Considering equal length of l_1 and l_5, as well as l_2 and l_4, the equation can be shortened and solved for l_6, as shown in Eq. 3. Table 1 lists the dimensions of the joint.

$$l_6 = l_2(\sin\gamma_1 + \sin\gamma_2) + l_3 * \sin\left(\cos^{-1}\left(\frac{l_1(\sin\gamma_1 + \sin\gamma_2)}{l_3}\right)\right) \quad (3)$$

Table 1. Geometry of the Joint

Variable	Value in mm
l_1 and l_5	30
l_2 and l_4	14
l_3	182.165

Using the average values of l_6 for a given bending angle, the required offset Δh to approximate a spherical rolling motion can be calculated:

$$\Delta h = \frac{{l_6}^2 - h^2}{4(h - \cos\alpha_2 * l_6)} \quad (4)$$

For the geometry of the designed joint, an offset of $\Delta h = -2{,}24$ mm is necessary to assume a spherical rolling motion within a range of $\alpha_2 = \pm 45°$. The shift of the center of rotation is visualized in Fig. 5.

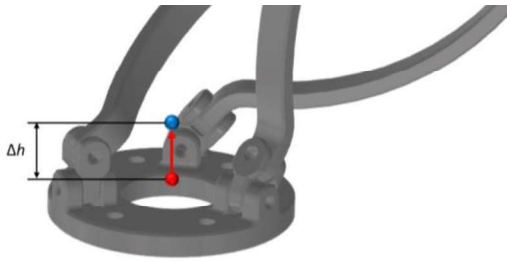

Fig. 5. To integrate the calculated offset into the design, the height of the individual joints was adjusted accordingly.

The resulting change in the deviation of the centre point distance is visualized in Fig. 6.

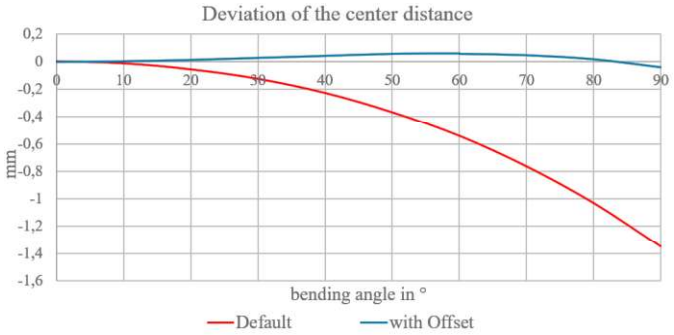

Fig. 6. The deviation of the distance between the virtual contact of the two spheres and the center of the joint was significantly reduced by calculating and implementing the offset of the center point.

When integrated into the design, the calculated offset results in a low deviation from an ideal rolling motion and therefore allows for the use of an antagonistic cable drive.

4. Design

4.1. Components

The main structure of the robot arm is currently additively manufactured using FDM technology with PLA material. In the future, to achieve a lightweight and buoyancy-neutral design, the structure will be produced using PA12 and PA12-CF. Dyneema® rope is selected for the tendons because of its high tensile strength and corrosion resistance. Self-lubricating bushings and ball bearings are employed to withstand the saltwater environment. The pressure resistance of individual components has been tested up to 600 bar over two 24-hour cycles.

4.2 Implementation

To actuate the joint, opposing cable pulls are positioned along the two axes of rotation. The previously calculated offset is implemented to ensure a constant tension on the tendons. To amplify the torque of the joint without the need for high maintenance gearboxes, a four to one reduction is integrated into the cable pulls, as shown in Fig. 7.

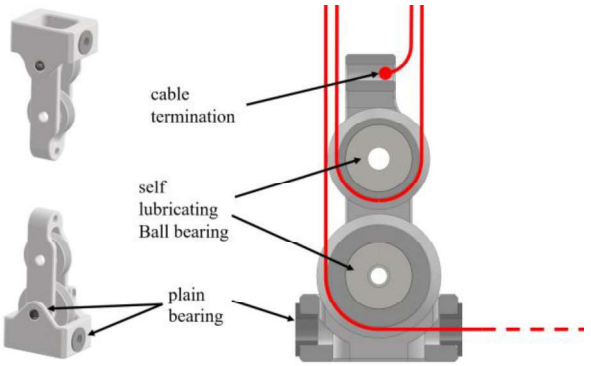

Fig.7. The four-to-one reduction implemented in the cable guides.

The flexibility of the main linkages in the joint enables it to adapt to external loads or obstacles. To maintain constant tension on the tendons, a spring-loaded tensioner is added to the design. This system compensates for any changes in length under load while ensuring a backlash-free connection between the motor and joint angle during normal operation.

5. Prototype

A prototype of the design was manufactured using PLA to test the concept's properties in a water basin environment. Bowden Tubes can be placed between the linkages to provide actuation for further joints that can be added at a later point. Carbon fiber reinforced tubes are used on the straight segments to increase the reach of the robot without adding unnecessary weight. The prototype is actuated by Brushless DC (BLDC) motors with magnetic encoders to avoid any moving electrical contact points and therefore allow for pressure neutral isolation against saltwater. Fig. 8 shows the completed prototype.

Fig. 8. For testing the design, a prototype of the (VRCJ) was manufactured primarily using PLA and carbon fiber-reinforced tubes. The tendon actuation system was implemented using two brushless DC motors.

Mechanical end-stops (depicted in Fig. 9) are integrated into the cable pulls. They provide a means of calibrating the position of the joint in relation to the magnetic encoders on the motor for each axis.

To calibrate the joint position after start up, the motor of the first axis moves continuously in one direction until it reaches a predefined resistance by pushing against the mechanical end-stop. The motor position is saved and the process repeated for all directions and axis. Afterwards the midpoint and reach for all axis can be calculated.

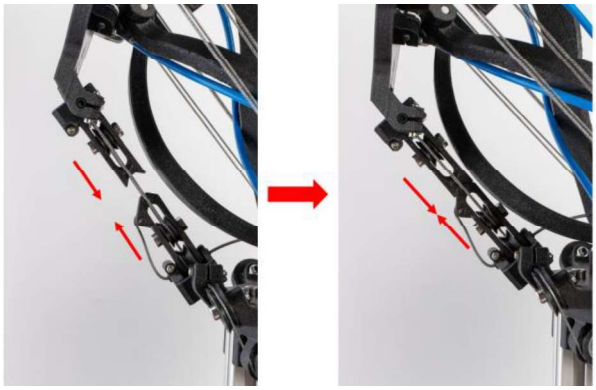

Fig. 9. The mechanical end stops calibrating of the tendon actuation.

6. Control

There are two methods for controlling the joint and thus the robot:

The first method involves the independent control of both rotations, which is suitable for joystick or master-slave system applications. In this approach, each axis of rotation is monitored by a separate controller, allowing the angle to be translated into the corresponding motor position through calculations based on changes in cable length. In Eq. 4 and Fig. 10 the relation between the bending angle of the joint and the cable length is described.

$$\Delta s = b * \cos(\alpha_2) \quad (5)$$

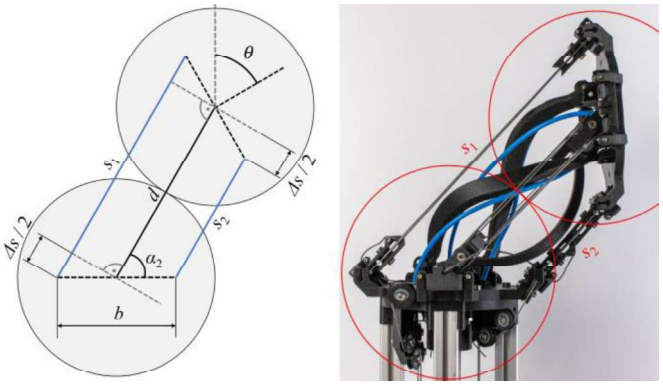

Fig. 10. Relation between bending angle and cable length.

The second option provides a combined description of the joint position using a bending plane and the bending angle along this plane. This approach allows the position to be translated into quaternion coordinates, as demonstrated by Kim et al. [6].

This method would be preferred for translating end effector coordinates into joint angles, for example when using autonomous programs to control the arm. Since the sediment sampler during the deployment of an ROV into the deep sea is controlled manually by an operator, the first method of control is preferred for its simplicity in this application.

7. Experimental Validation

To evaluate the repeatability of the previously described homing sequence, joint positions are monitored using an OptiTrack® system. The resulting positions following the calibration sequence are compared to validate the method of detecting mechanical end-stops via motor torque. Fig. 11 shows the measured rotation of the joint during one calibration cycle. Note that the starting positions of the joint are chosen randomly to better mimic real word conditions. Repeated measurements demonstrated that the calibration technique used provides sufficient precision. However, the tests revealed that the cogging torque of the BLDC motors resulted in some inaccuracies. This issue can be addressed by replacing the motors.

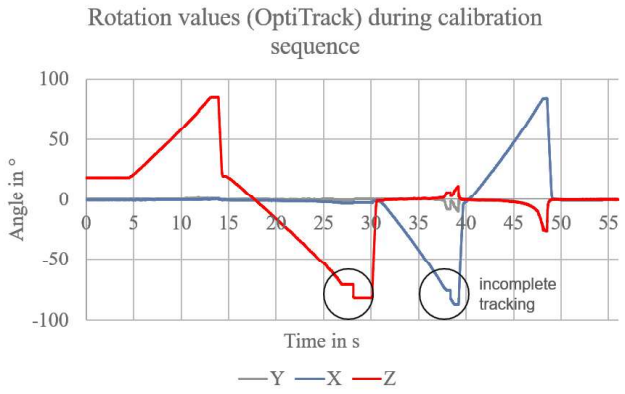

Fig. 11. The rotation of the joint during the calibration.

To test the influence of different components and the water-resistance on the required motor-torque, a simple motion sequence was repeated for different setups of the robot.

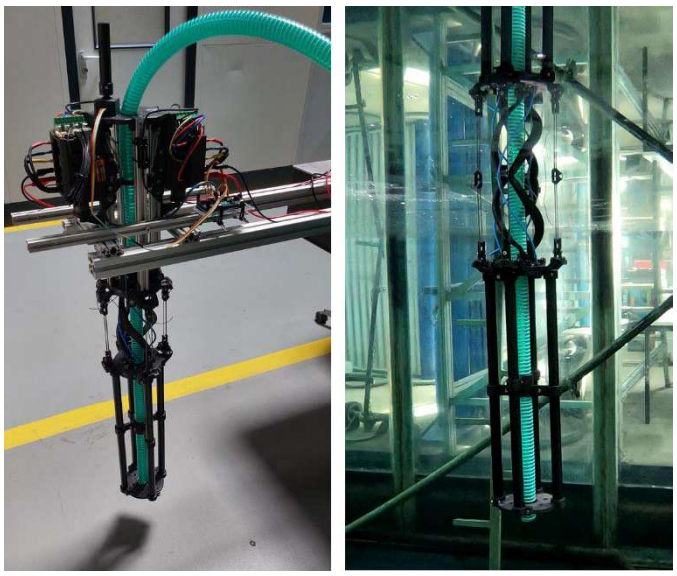

Fig. 12. Test setup of the Prototype outside and inside water

The results in Fig. 13 show a notable increase in motor torque due to the stiffness of the vacuum conduit. Although, the water resistance further increased the torque during motion, it positively affected the holding torque due to the almost buoyancy neutral construction of the robot.

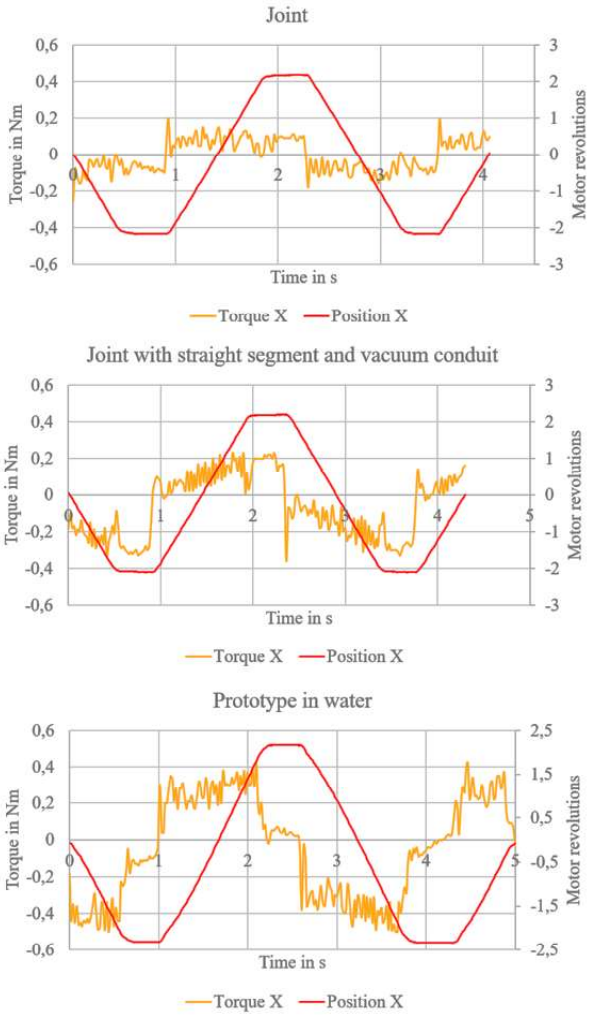

Fig. 13. The motor torque was measured under three different conditions.

To assess the final weight of the robot, the weight of the single modules like the joints or drive units was calculated under the utilization of PA-12 and PA-12 CF for the main components. A potential configuration of two joint and three straight segments (as shown in Fig. 14) and a reach of 1.5 m was used as a reference.

Table 2. Calculated weight of the robot modules

Module / Configuration	Amount	Volume	Weight in air	Weight in water
		cm^3	g	g
Straight segment (0,45 m)	1	300,78	352,10	43,80
Joint	2	442,03	508,27	55,19
Straight segment with cable guide (0,45 m)	2	365,41	433,01	58,47
Dyneema rope (2 m)	16	1,89	1,80	-0,14
Vacuum conduit (1,5 m)	1	312,50	375,00	54,69
Drive Unit	4	583,43	1295,95	697,94
Sum of Arm Config. (no drive)		2258,47	**2638,45**	**323,52**
Sum of complete Arm		4592,19	7822,27	3115,27

Assuming the drive units are positioned inside the ROV, the external segments of the robot only result in a very low weight of 324 g in water or 2.64 kg in air, as shown in Table 2. For comparison: traditional hydraulic manipulators used for suction sampling weigh between 68 kg and 181 kg [7].

As the previous experiments have shown, smaller motors with a slightly lower maximum torque would be sufficient to actuate the robot. Therefore, a significant weight reduction in the drive units is possible.

8. Conclusion

Based on the selected Virtual Rolling Contact Joint, a concept for a modular robot arm design was developed. The joint was mathematically modeled, and the necessary geometry for an antagonistic cable guide was calculated. Pressure-neutral and corrosion-resistant materials and components were chosen to implement the developed concept, facilitating a lightweight construction that is as buoyancy-neutral as possible. For the final implementation, components will be manufactured from PA12 and PA12-CF using SLS printing. Various components such as glass ball bearings and carbon fiber tubes were experimentally tested for their pressure resistance.
Using the selected components, a prototype of the joint was additively manufactured from PLA. This prototype was then equipped with drives and a controller. Testing was conducted on the repeatability of the calibration, as well as on the drive force when operating the joint with a vacuum hose in both air and water. The design's functionality was successfully demonstrated using the prototype.

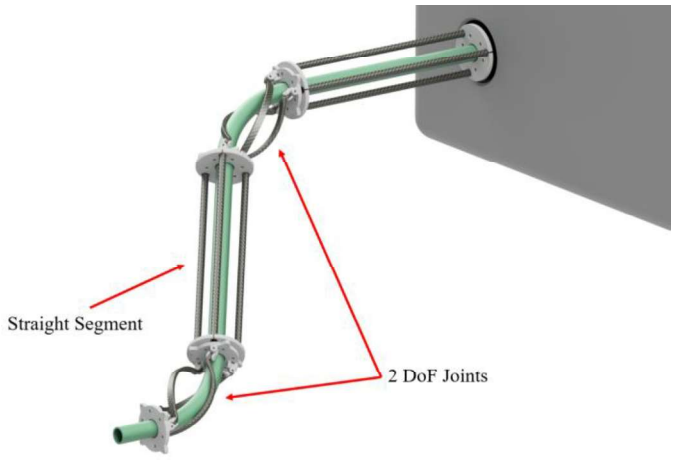

Fig. 14. The final robot configuration concept

An evaluation of the weight, using final materials, indicates that the robot arm is exceedingly light at just 2.64 kg and can be made completely buoyancy-neutral through the integration of small buoyancy modules. The mass of the drives, at 5.18 kg, is also low compared to existing solutions and can be mounted either on the side or inside the ROV.

In conclusion, this work has developed and tested a joint for the modular design of a corrosion-resistant, buoyancy- and pressure-neutral robotic arm intended for sediment sampling. The robotic arm features a remarkably low moving mass due to the displacement of the drives while maintaining a long reach, making it suitable for integration with ROVs of various sizes.

Future work will involve constructing the next iteration of the prototype as shown in Fig. 14, with enhancements aimed at waterproofing the design for comprehensive underwater testing. Another objective is to transition from manual steering of the suction sampling system to an automated approach, which could significantly expedite the sampling process.

Acknowledgements

The ASDDSA Project is under by the Deutsche Forschungsgemeinschaft (DFG, German Research Foundation) under grant no. 498342743.

References

[1] Huneke H, Mulder T. Deep-Sea Sediments. Elsevier; 2011.

[2] Capocci R, Dooly G, Omerdić E, Coleman J, Newe T, Toal D. Inspection-Class Remotely Operated Vehicles—A Review. J Mar Sci Eng 2017;5:13. https://doi.org/10.3390/jmse5010013.

[3] Peters J, Sourkounis CM, Wiese M, Kwasnitschka T, Raatz A. Single Channel Soft Robotic Actuator Leveraging Switchable Strain-Limiting Structures for Deep-Sea Suction Sampling. 2023 IEEE/RSJ International Conference on Intelligent Robots and Systems (IROS), IEEE; 2023, p. 6484–90. https://doi.org/10.1109/IROS55552.2023.10341262.

[4] Sourkounis CM, Morales DSG, Kwasnitschka T, Raatz A. Hard Shell, Soft Core: Binary Actuators for Deep-Sea Applications. 2024 IEEE International Conference on Robotics and Automation (ICRA), IEEE; 2024, p. 9355–61. https://doi.org/10.1109/ICRA57147.2024.10610349.

[5] Sourkounis CM, Kwasnitschka T, Raatz A. Tendon-Driven Continuum Robot for Deep-Sea Application. 2024 IEEE International Conference on Robotics and Automation (ICRA), IEEE; 2024, p. 1498–504. https://doi.org/10.1109/ICRA57147.2024.10611177.

[6] Kim Y-J, Kim J-I, Jang W. Quaternion Joint: Dexterous 3-DOF Joint Representing Quaternion Motion for High-Speed Safe Interaction. 2018 IEEE/RSJ International Conference on Intelligent Robots and Systems (IROS), IEEE; 2018, p. 935–42. https://doi.org/10.1109/IROS.2018.8594301.

[7] Subsea Manipulator Systems. Https://WwwTechnipfmcCom/En/What-We-Do/Subsea/Robotics/Manipulator-Systems/ n.d.